

Advanced Lab Course: Particle Physics

CP-Violation

Leander Flottau

leander.flottau@tu-dortmund.de

Ajeesh Garg

smajgarg@tu-dortmund.de

25. June 2024

TU Dortmund University – Department of Physics

Contents

1	Introduction	3
2	Large Hadron Collider	3
3	Construction of LHCb	4
3.1	Vertex Locator	4
3.2	Tracking System	4
3.3	Calorimeter System	5
3.4	Particle Identification Detectors (RICH1 and RICH2)	5
3.5	Muon System	5
3.6	Online and Offline Data Processing	6
4	Analysis	7
4.1	Simulation	7
4.2	Real data	7
4.2.1	Preselection	7
4.2.2	Initial measurement of the CP-Violation	9
4.2.3	Removing intermediate resonances	9
4.2.4	Local CP-violation	11
5	Conclusion	13
	References	14

1 Introduction

The Standard Model (SM) of particle physics is a highly successful theoretical framework that has been able to explain the most fundamental interactions of nature. Over the past century, it has been rigorously tested and its accuracy of predictions that have been confirmed through numerous experiments.

Despite its successes, the Standard Model is not a complete theory. Several fundamental questions still remain unanswered, such as the nature of dark matter and dark energy as well as the observed matter-antimatter asymmetry in the universe. This matter-antimatter asymmetry is particularly intriguing because the Big Bang should have produced equal amounts of matter and antimatter, yet our observable universe is overwhelmingly composed of matter.

Under Sakharov conditions, a crucial aspect of this asymmetry is CP Violation, which refers to the violation of the combined symmetries of charge conjugation (C) and parity (P). CP Violation has been observed in the decays of certain particles and is incorporated into the SM through the complex phase of the Cabibbo-Kobayashi-Maskawa (CKM) matrix. However, the extent of CP Violation predicted by the SM is insufficient to account for the baryon asymmetry observed in the universe, suggesting the presence of new physics beyond the Standard Model.

This mechanism of CP Violation was further verified experimentally in the weak B Meson decays by the *Barbar* (1999) and *Belle* experiments (2010) but the amount of CP violation observed is still too small to account for matter-antimatter asymmetry of the universe. The large Hadron collider beauty (LHCb) experiment is designed specifically to measure this CP violation more precisely in the case of rare decays of hadrons containing bottom and charm quarks.

This report focuses on the measurement of CP Violation in the decays of B mesons (particles containing a bottom quark) using data collected by the LHCb experiment. By comparing the decay rates of B^+ mesons and their antiparticles (B^-) into three hadrons, we aim to quantify the CP asymmetry. Specifically, we analyze decays producing three kaons, which are less affected by background noise compared to those involving pions.

The results from this analysis will contribute to the broader effort to uncover the mechanisms behind CP-violation and explore potential New Physics that could explain the observed matter-antimatter asymmetry in the universe.

2 Large Hadron Collider

The Large Hadron Collider (LHC) at CERN, near Geneva, is a particle accelerator that collides proton beams at a centre-of-mass energy of 7 TeV. Each beam contains approximately 2000 bunches, each with about 1.1×10^{11} protons, colliding at an average rate of 15 MHz, resulting in numerous inelastic interactions. The main goal of the LHC experiments is to test the Standard Model of particle physics and to search for physics beyond SM.

The LHCb experiment is one of the four main experiments at the LHC, specifically

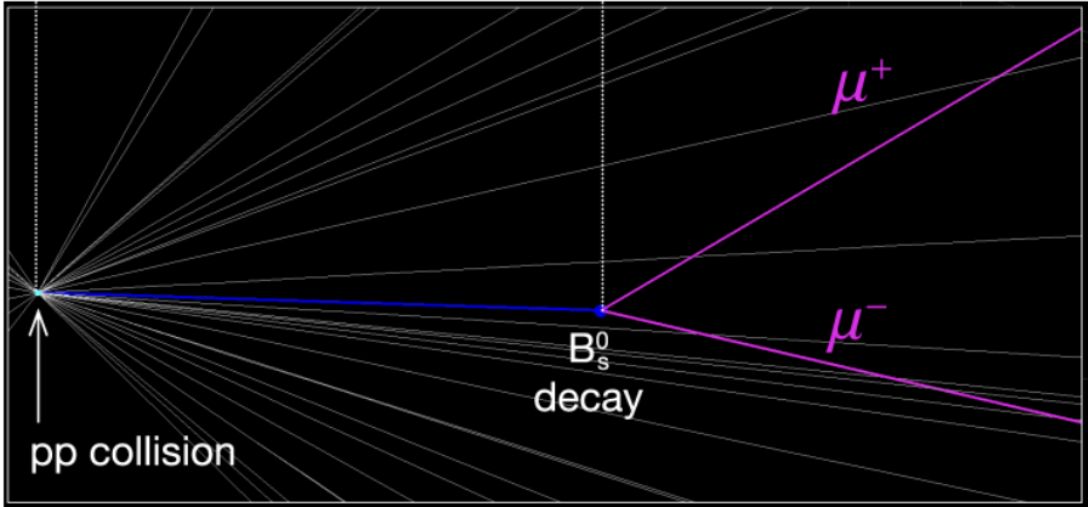


Figure 1: Schematic depiction of a proton-proton interaction followed by a B-decay [1]

designed to study CP-violation and the rare decays of hadrons containing b and c quarks. The detector is positioned at the LHC's interaction point 8 (IP8) and features a single-arm forward spectrometer. This design is optimized to capture particles produced in the forward direction, where b quarks are predominantly emitted following proton-proton collisions.

3 Construction of LHCb

The LHCb detector is made up of several components serving different functions in the particle detection process. A schematic depiction of the detector and all of its components can be viewed in 2.

3.1 Vertex Locator

The Vertex Locator (VELO) is crucial for reconstructing the primary vertex, where the initial proton-proton collisions occur, and secondary vertices, where short-lived particles decay. The VELO consists of silicon strip detectors arranged in close proximity to the interaction point. These detectors provide high-resolution measurements of particle trajectories, allowing precise determination of vertex positions.

3.2 Tracking System

The tracking system of LHCb includes a dipole magnet and several tracking stations. The dipole magnet creates a magnetic field that bends the tracks of charged particles. By measuring the curvature of these tracks, the momenta of the particles can be calculated.

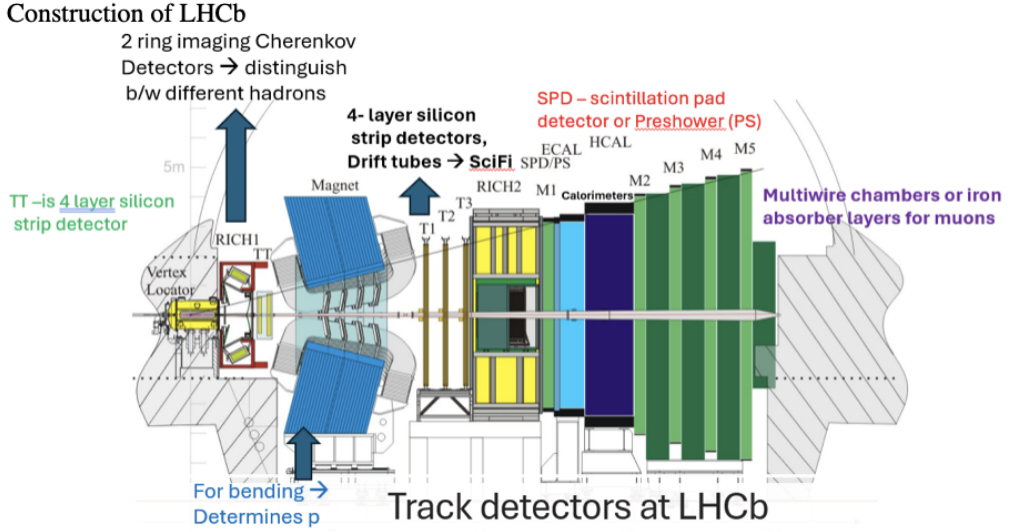


Figure 2: Schematic depiction of the LHCb detector [1]

The tracking stations, positioned before and after the magnet, consist of silicon strip detectors and straw drift tubes, which detect charged particles and their trajectories.

3.3 Calorimeter System

The calorimeter system of LHCb is designed to measure the energy of photons, electrons, and hadrons. It consists of the Scintillating Pad Detector (SPD), the Preshower Detector (PS), the Electromagnetic Calorimeter (ECAL), and the Hadronic Calorimeter (HCAL). The ECAL absorbs the electromagnetic particles while the HCAL absorbs the hadrons and hence, their energy is determined. The ECAL uses lead as the material while HCAL uses iron as the material.

3.4 Particle Identification Detectors (RICH1 and RICH2)

Two Ring-Imaging Cherenkov (RICH) detectors are used for particle identification. RICH1 is located upstream of the magnet, and RICH2 is downstream. These detectors exploit the Cherenkov effect, where charged particles traveling faster than the speed of light in a medium emit light at a characteristic angle. By measuring this angle, the velocity of the particle can be determined. This allows for the calculation of the particle mass which can be used to determine the particle type.

3.5 Muon System

The muon system consists of alternating layers of iron and multi-wire proportional chambers. Muons, unlike most other particles, can penetrate the dense iron layers,

allowing them to be identified and tracked. This system is essential for studying decays that produce muons in the final state.

3.6 Online and Offline Data Processing

The LHCb detector produces a vast amount of data, which is filtered and processed in real-time by an online trigger system. This system selects events of interest and reduces the data volume for further analysis. Selected events are then sent to an offline computing grid, where detailed analyses are performed.

4 Analysis

When trying to effectively measure CP-Violation the measurement first has to be cleared of combinatorial background as well as intermediate resonances. The latter can be achieved by using a dalitz plot.

4.1 Simulation

Siimulations of events are useful to visualize the characteristics of the $B \rightarrow KKK$ decay. The data used here contains 50000 simulated B decays who are a pure signal sample without background or resonances. Figure 3 shows the individual components

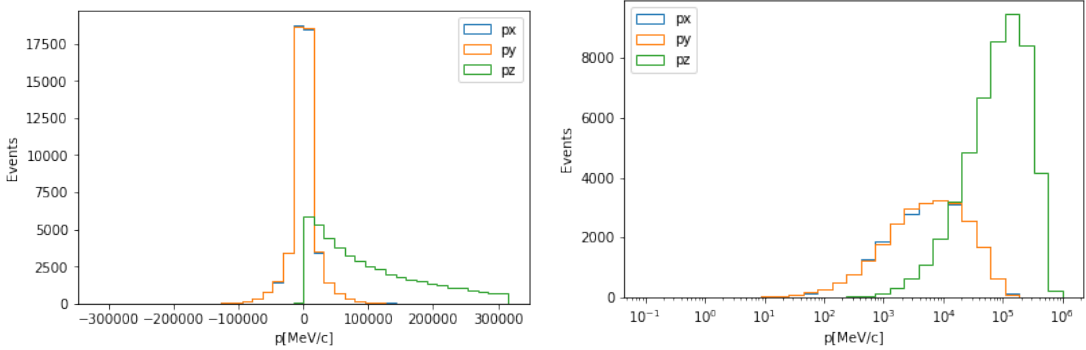


Figure 3: Components of the momentum of the first detected Kaon.

of the momentum of the first Kaon in the simulation. While the distributions of the x- and y-components are almost identical and symmetric around 0 the z-component contains no negative values because of the structure of the detector. The log-scaled plot illustrates, that the events from this decay are strongly forward boosted resulting in the high momentum in the z-direction. Assuming, that the Energy and the momentum is conserved in the decay those quantities can be calulalted for the initial B-meson. Using the relativistic energy-momentum-relation

$$E^2 = p^2 + m^2 \quad (1)$$

the invariant mass of the B-meson is determined. The resulting spectrum shows a clear peaking structure around the expected theoretical value $m_B = 5279 \pm 0,07$ [2] as seen in Figure 4.

4.2 Real data

4.2.1 Preselection

CP-violation is measured here using a dataset containing data of the LHCb detector. Those events are already prefiltered by the detector triggers but still contain a lot of combinatorial background. As the mass plot 5 shows the background events still make

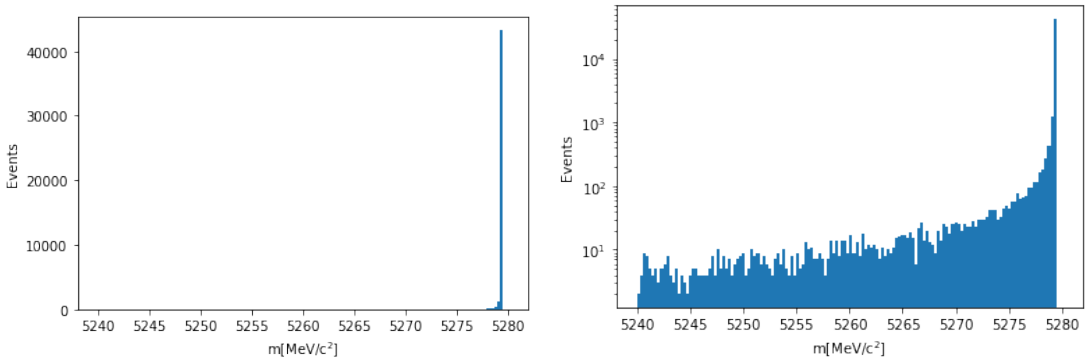


Figure 4: Invariant mass of the B-meson according to the simulation on a linear scale (left) and a logarithmic scale (right).

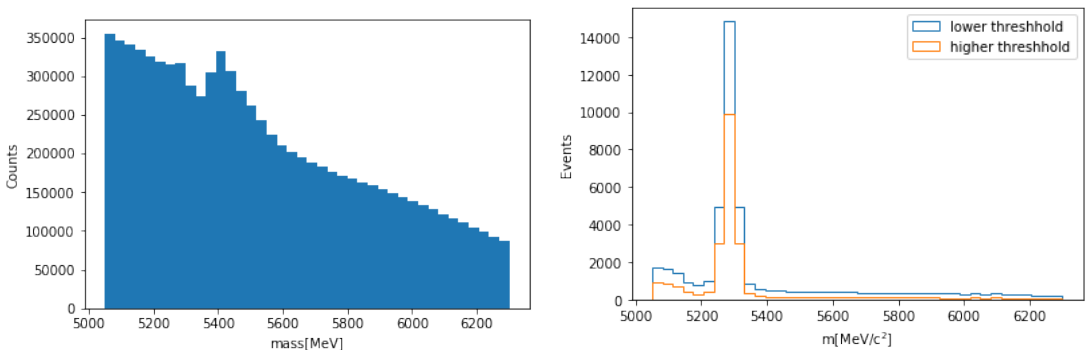


Figure 5: Mass of the B-meson for the unfiltered data (left) and the filtered data (right)

up a majority of the data. To fix this the data has to be preprocessed using features provided in the set that are precalculated and contain information whether a measured event was a muon and how likely it is to be a Kaon P_K or a pion P_π . Imposing two different selections based on the thresholds $T_{1K} = T_{1\pi} = 0.5$ and $T_{2K} = 0.65/T_{2\pi} = 0.35$. This requires events to have Probability to be a pion of at most T_K and a probability of being a pion of at least T_π . The selected events for both cuts are shown in Figure 5, while both selections filter for the required mass peak very well, they differ in how much background they cut and how much of the peak they preserve. For the following analysis we are using the lower threshold. Additionally the total mass range is restricted for the further analysis steps to $5235 \text{ MeV} < m_B < 5335 \text{ MeV}$

4.2.2 Initial measurement of the CP-Violation

Using the filtered data the global CP-asymmetry, defined as:

$$A = \frac{N^+ - N^-}{N^+ + N^-} = 0.0516 \quad (2)$$

as well as the uncertainty of the asymmetry:

$$\sigma_A = \sqrt{\frac{1 - A^2}{N^+ + N^-}} = 0.0063 \quad (3)$$

can be calculated. The number of positively charged B -mesons N^+ and the number of negatively charged B -mesons N^- are determined by splitting the data based on the sum of the charges of the decay products. Based on these values the significance of the measurement can be determined:

$$\alpha = \frac{A}{\sigma_A} = 8.16 \quad (4)$$

which corresponds to a discovery.

Additionally to the statistical uncertainty the measurement also contains systematic uncertainties for several reasons. Because the initial state in a proton-proton-collision is not exactly known the production rate of B^+ and B^- differ resulting in an asymmetry unrelated to CP violation. This natural asymmetry amounts to a total of 1%. This asymmetry has to be considered as an additional uncertainty to the calculated global asymmetry. Considering this factor results in a significantly higher overall uncertainty of $\sigma_A = 0.012$ reducing the significance to $\alpha = 4.362\sigma$ which only corresponds to an observation as opposed to a discovery.

4.2.3 Removing intermediate resonances

The decay of the B -meson can produced through so called resonances when two of the three final state particles stem from an intermediate particle. Of the three possible combinations of two of the final state particles only the the two combinations where the combined charge vanishes allow for such resonances. By constructing the invariant

masses of those two particle combinations and plotting them against each other in a so called Dalitz-plot these intermediate resonances can be identified as 'bands' of events in the plot. A Dalitz-plot for an ideal B-decay is presented in figure 6 generated from the

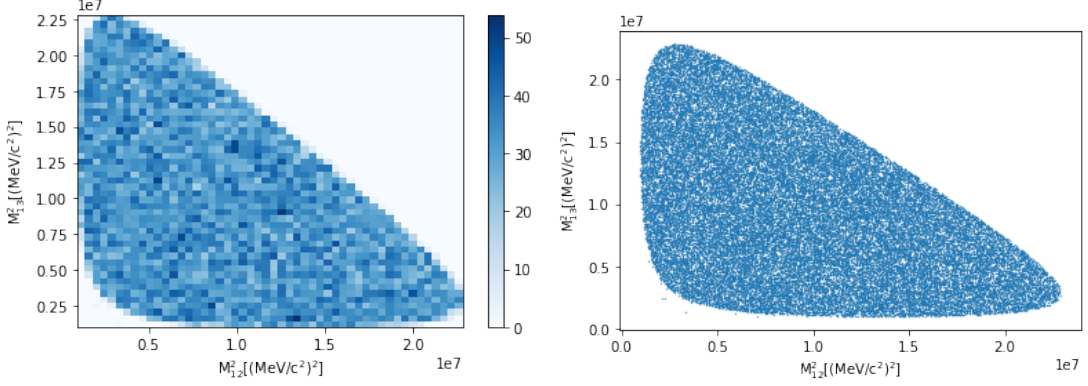


Figure 6: Dalitz-plot of the simulated data as a histogram (left) and a scatter-plot (right)

simulation where events are evenly distributed across the kinematic region of the decay. When utilizing the real data the resulting plot is displayed in 7. This already shows

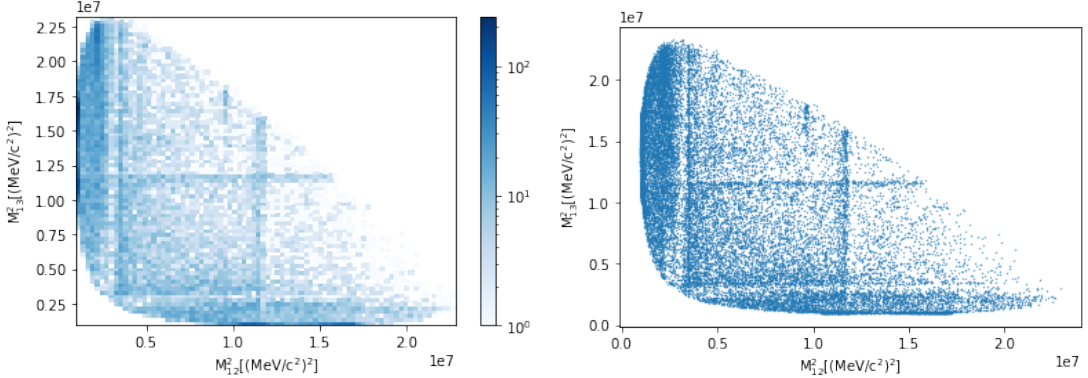


Figure 7: Dalitz-plot of the real data as a histogram (left) and a scatter plot (right)

outlines of some kinematic regions which are more densely populated.

To improve the visibility of the plot, the two resonances in every individual event are sorted by their invariant mass. This is possible because both resonances are made up of the same particles so they can be assumed to have the same distribution. By ordering the resonances the range on both axes reduces hence increasing the density of events in the plot. The sorted Dalitz-plot is shown in figure 8. The most notable resonance is a densely populated band of events at a mass of about 1860 MeV. This resonance can be attributed to the D_0 -meson which has an invariant mass of $m_{D_0} = (1864.84 \pm 0.05)$ MeV [2]. The D_0 is a charmed meson and therefore the events proceeding through this resonance have

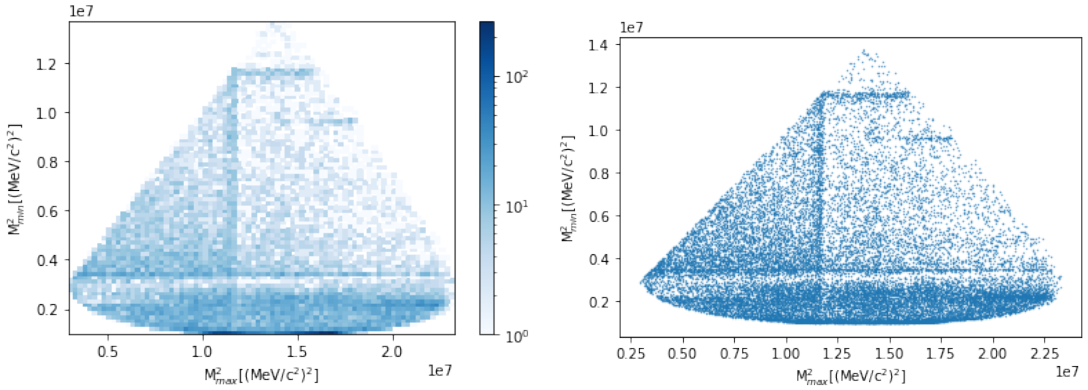


Figure 8: Dalitz-plot of the real data after sorting the resonances as a histogram (left) and scatter plot (right)

to be filtered out by rejecting the events in the corresponding kinematic region visible as a band in the Dalitz-plot. The Dalitz plot after removal of the resonance band is

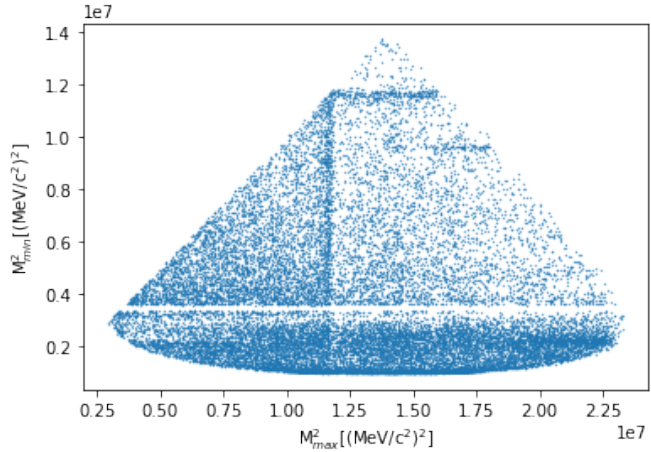


Figure 9: Dalitz plot after removing the events from the D^0 resonance band

displayed in 9.

4.2.4 Local CP-violation

To improve the significance of the measured CP-violation it can be viewed locally in the different kinematic regions of the Dalitz-plot. The resulting asymmetries and the total differences between positive and negative events are displayed in 10. A small number of bins, that had a very low total event count and either no positive events or no negative events were discarded for this analysis because they produce unrealistically high significances. Using this the uncertainty including the systematic component and consequently the significance of the measured CP-violation can be calculated (11). It can

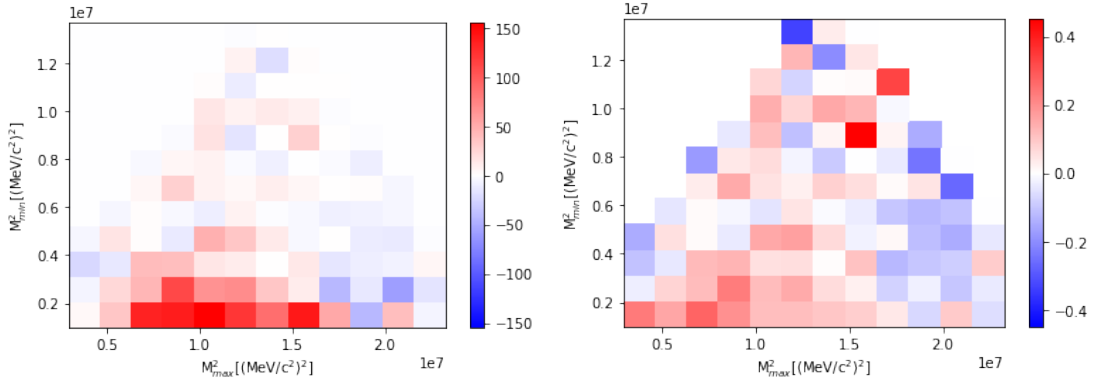


Figure 10: Difference between B^+ and B^- events (left) and local asymmetry (right) in different kinematic regions of the dalitz plot

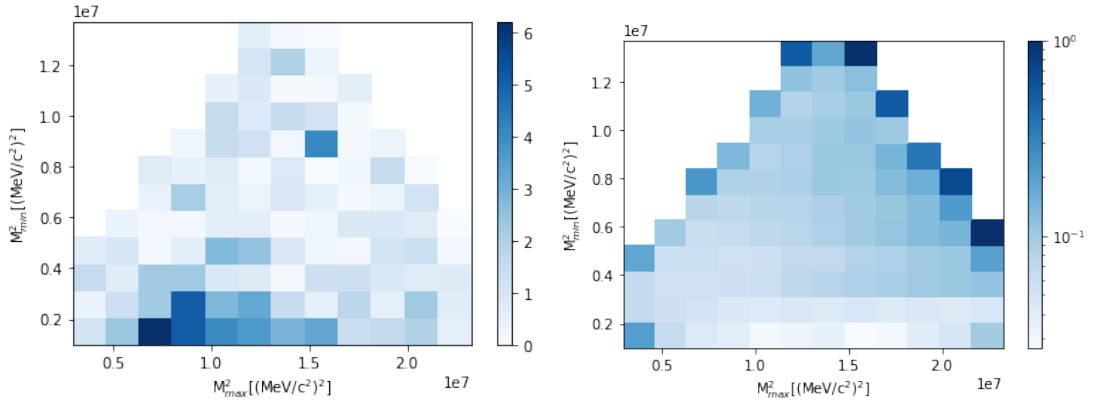


Figure 11: Significance of the measured CP-violation based on the kinematic region.

be seen that there is a region of 5 bins with high asymmetries and low significances in the third to sixth M_{max} -bins and the first M_{min} -bin and in the fourth M_{max} -bin and second M_{min} -bin. When only considering the data from those bins we get an asymmetry of:

$$A = 0,1645 \pm 0,0184 \quad (5)$$

which amounts to a significance of $\alpha = 8,92\sigma$. So unlike in the global case the local

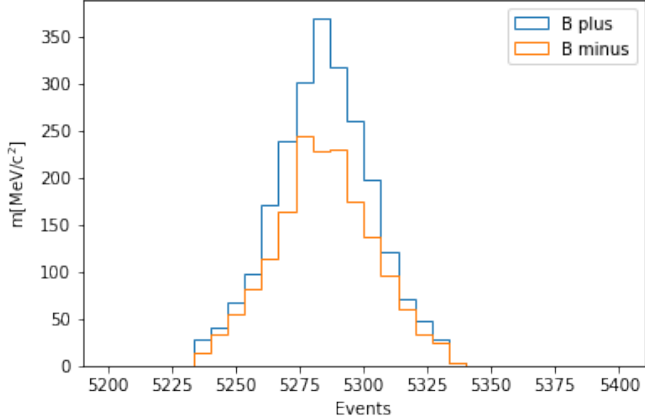


Figure 12: Reconstructed mass of the B-meson in the selected kinematic region.

asymmetry can be considered a discovery. The mass distributions of the B^+ and B^- in the selected region can be viewed in 12.

5 Conclusion

The data provided by the Lhcb experiment allows for the discovery of CP-violation by measuring the global matter-antimatter asymmetry $A_{\text{global}} = 0.0516 \pm 0.0063$ which corresponds to a high significance of more than 8σ when only considering statistical uncertainties. However when considering the systematic uncertainties imposed by the imbalanced nature of proton-proton-collisions this significance reduces to $4,326\sigma$ showing that on this scale the problem is dominated by systematic rather than statistical uncertainties.

To improve the significance of the measurement the intermediate D_0 -resonance, which is clearly visible in the Dalitz-plots, has to be removed to be able to search for CP-violation locally. Using this principle the local Asymmetry in the most significant region $A_{\text{local}} = 0,1645 \pm 0,0184$ can be determined with a high significance of $\alpha = 8,92\sigma$ considering systematic uncertainties which corresponds to a discovery.

In a more precise analysis of the CP-violation other systematic contributions to the uncertainty like the effect of the detector itself on the measurement would have to be considered. Another potential problem is posed by the imperfect signal-background selection due to the fact that the thresholds set in this preselection could not be set very high to achieve a high sample purity because the size of the dataset is not sufficient.

References

- [1] *Measurements of matter-antimatter asymmetries with the LHCb experiment.* Fakultät Physik, TU Dortmund. 2022.
- [2] R. L. Workman et al. “Review of Particle Physics”. In: *PTEP* 2022 (2022), p. 083C01. DOI: [10.1093/ptep/ptac097](https://doi.org/10.1093/ptep/ptac097).